J|A|C|S
ARTICLES
Published on Web 12/07/2006

Catalytic Mechanism of Glycosyltransferases: Hybrid Quantum Mechanical/Molecular Mechanical Study of the Inverting *N*-Acetylglucosaminyltransferase I

Stanislav Kozmon and Igor Tvaroška*

Contribution from the Institute of Chemistry, Slovak Academy of Sciences, 845 38 Bratislava, Slovak Republic

Received August 16, 2006; E-mail: chemitsa@savba.sk

Abstract: The Golgi glycosyltransferase, *N*-acetylglucosaminyltransferase I (GnT-I), catalyzes the transfer of a GlcNAc residue from the donor UDP-GlcNAc to the C2-hydroxyl group of a mannose residue in the trimannosyl core of the $Man_5GlcNAc_2-Asn-X$ oligosaccharide. The catalytic mechanism of GnT-I was investigated using a hybrid quantum mechanical/molecular mechanical (QM/MM) method with a QM part containing 88 atoms treated with density functional theory (DFT) at the BP/TZP level. The remaining parts of a GnT-I complex, altogether 5633 atoms, were modeled using the AMBER molecular force field. A theoretical model of a Michaelis complex was built using the X-ray structure of GnT-I in complex with the donor having geometrical features consistent with kinetic studies. The QM(DFT)/MM model identified a concerted S_N2-type of transition state with D291 as the catalytic base for the reaction in the enzyme active site. The TS model features nearly simultaneous nucleophilic addition and dissociation steps accompanied by the transfer of the nucleophile proton H_b2 to the catalytic base D291. The structure of the TS model is characterized by the O_b2-C1 and $C1-O1$ bond distances of 1.912 and 2.542 Å, respectively. The activation energy for the proposed reaction mechanism was estimated to be ~19 kcal mol^{-1}. The calculated α-deuterium kinetic isotope effect of 1.060 is consistent with the proposed reaction mechanism. Theoretical results also identified interactions between the H_b6 and β-phosphate oxygen of the UDP and a low-barrier hydrogen bond between the nucleophile and the catalytic base D291. It is proposed that these interactions contribute to a stabilization of TS. This modeling study provided detailed insight into the mechanism of the GlcNAc transfer catalyzed by GnT-I, which is the first step in the conversion of high mannose oligosaccharides to complex and hybrid *N*-glycan structures.

1. Introduction

Understanding the structural origin of the catalytic efficiency of enzymes is a fundamental goal and challenge in biological science. Theoretical studies of enzyme-catalyzed reactions have recently received much attention because they provide detailed information at the microscopic level.[1−3] Early gas-phase molecular modeling studies using simple models were useful in terms of gaining insights, but it is now clear that nearby environmental effects of protein must be included in some way. One simple approach is just to consider some of the key residues in the calculations with some atom fixed at their crystallographic positions. The development of several hybrid methodologies[4,5] (where only a part of the system is described by quantum mechanics (QM) while the rest is usually considered by means of molecular mechanics (MM)) has allowed the inclusion of larger parts of the protein environment into the study of the reaction mechanism and might provide more detailed insight into the catalytic mechanism of enzymes.

Glycosyltransferases are involved in the biosynthesis of glycans, which play important roles in many biological events[6] and are potentially promising targets for inhibition, possibly leading to therapeutic compounds. These enzymes attach a sugar molecule to a specific acceptor, thus creating a glycosidic linkage.[7] A comparison of structures of inverting glycosyltransferases belonging to the GT-2 SpsA family,[8] also identified as the "GT-A" superfamily according to the CAZY nomenclature,[9] has shown the existence of conserved catalytic and recognition machinery. Many aspects of the functions and catalytic mechanisms of glycosyltransferases are, however, still unknown. *N*-Acetylglucosaminyltransferase I (UDP-*N*-acetyl-D-glucosamine: α-3-D-mannoside β-1,2-*N*-acetylglucosaminyltransferase I, GnT-I, EC 2.4.1.101) is an inverting family 13 glycosyltransferase that catalyzes the transfer of a GlcNAc residue (2-acetamido-2-deoxy-α-D-glucopyranose) from the nucleotide-sugar donor

(1) Gao, J.; Truhlar, D. G. *Annu. Rev. Phys. Chem.* **2002**, *53*, 467−505.
(2) Garcia-Viloca, M.; Gao, J.; Karplus, M.; Truhlar, D. G. *Science* **2004**, *303*, 186−195.
(3) Truhlar, D. G.; Gao, J.; Alhambra, C.; Garcia-Viloca, M.; Corchado, J.; Sanchez, M. L.; Villa, J. *Acc. Chem. Res.* **2002**, *35*, 341−349.
(4) Gao, D. Q.; Pan, Y. K.; Byun, K.; Gao, J. L. *J. Am. Chem. Soc.* **1998**, *120*, 4045−4046.
(5) Maseras, F.; Morokuma, K. *J. Comput. Chem.* **1995**, *16*, 1170−1179.
(6) Varki, A. *Glycobiology* **1993**, *3*, 97−130.
(7) Schachter, H. *Curr. Opin. Struct. Biol.* **1991**, *1*, 755−765.
(8) Tarbouriech, N.; Charnock, S. J.; Davies, G. J. *J. Mol. Biol.* **2001**, *314*, 655−661.
(9) Coutinho, P. M.; Deleury, E.; Davies, G. J.; Henrissat, B. *J. Mol. Biol.* **2003**, *328*, 307−317.

10.1021/ja065944o CCC: $33.50

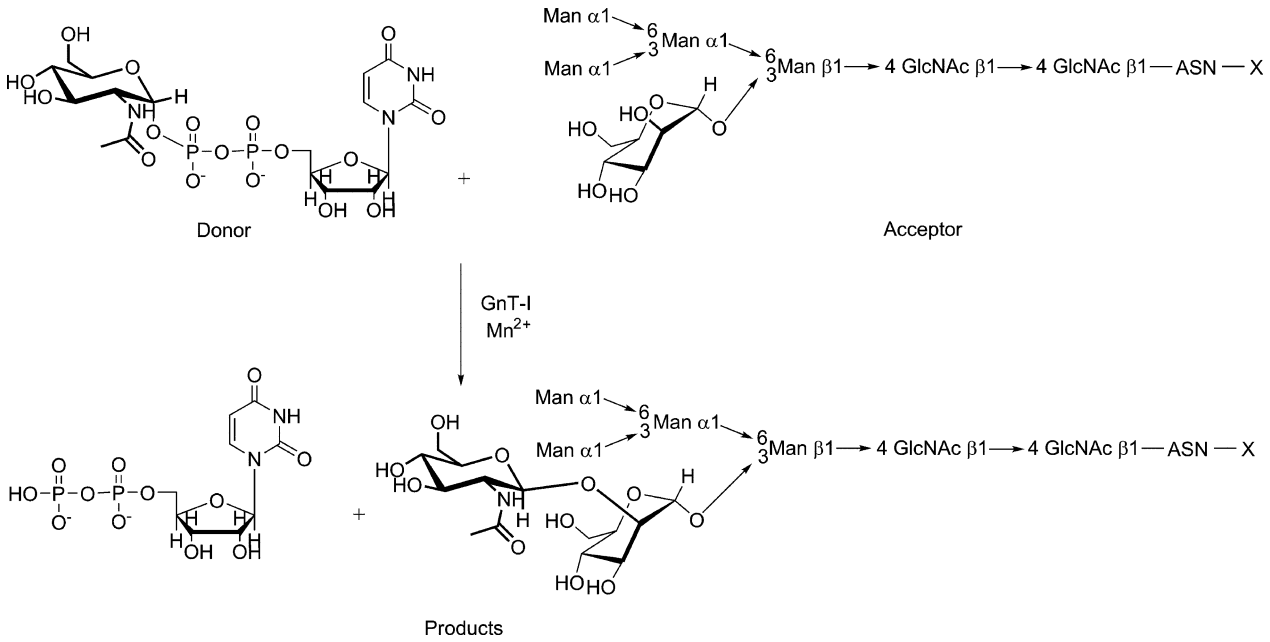

Figure 1. Schematic diagram of the enzymatic reaction catalyzed by GnT-I.

UDP-GlcNAc [uridine 5′-(2-acetamido-2-deoxy-α-D-glucopyranosyl pyrophosphate)] to the acceptor, which is the C2-hydroxyl group of a mannose residue in the trimannosyl core of the $Man_5GlcNAc_2-Asn-X$ oligosaccharide (Figure 1).[10] The attachment of the GlcNAc sugar is the first step in the biosynthesis of hybrid and complex N-linked glycans.[7] The transfer reaction of the GlcNAc residue occurs in the Golgi apparatus and can be regarded as a nucleophilic displacement of the UDP (uridine 5′-pyrophosphate) functional group at the anomeric carbon C1 of the GlcNAc residue of UDP-GlcNAc by the hydroxyl group at the C2 of the oligosaccharide acceptor. The crystal structure of the catalytic domain of rabbit GnT-I was determined[11] in *apo* form, in complex with UDP-GlcNAc/Mn^{2+}, and more recently in complex with donor substrate analogues[12] (PDB codes: 1FO8, 1FO9, 1FOA, 2AM3, 2AM4, 2AM5, and 2APC). The fold of GnT-I belongs to a superfamily named GT-A. Both the presence of the DxD motif (or its variants) and the requirement of a divalent cation for their activity are general features of the enzymes this family. In the case of GnT-I, the essential catalytic site is comprised of the catalytic base D291; one carboxylate D144, involved in the stabilization of the uracil; three carboxylate residues ^{211}EDD^{213}, forming the DxD motif; and the bound Mn^{2+} metal ion. Experiments have shown that GnT-I follows an ordered sequential *Bi Bi* kinetic mechanism,[10] where the enzyme first binds to both the metal cofactor and UDP-GlcNAc and subsequently to the $Man_5GlcNAc_2-Asn-X$ oligosaccharide acceptor. The oligosaccharide product, $GlcNAcMan_5GlcNAc_2-Asn-X$, is then released, followed by UDP.

This study is a continuation of our effort to explore the catalytic mechanism of glycosyltransferases. Previously performed high-level quantum mechanical calculations using simple models of glycosyltransferases[13−15] gained some insight into the microscopic characteristics of their enzymatic reaction and suggested that the catalytic mechanism involving a single catalytic base is energetically preferred over mechanisms using both a catalytic base and a catalytic acid for the reaction.[15] These findings are supported by all currently available X-ray crystal structures of inverting glycosyltransferases.[8,11,12,16−24] DFT calculations using the truncated 127 atoms active site model,[13] based on the X-ray crystallographic structure[11] of GnT-I, revealed one transition state associated with a reaction pathway following a concerted mechanism. Although these calculations provide very useful information about the catalytic reaction, consideration of the full relaxed system (substrates plus glycosyltransferase) could prove to be decisive in obtaining more realistic descriptions of their reaction mechanism. In this paper, to bridge this gap, we investigated the reaction catalyzed by GnT-I and employed the hybrid QM(DFT)/MM methodology, in which the full system (GnT-I plus substrates) is allowed to relax. This work is, to the best of our knowledge, the first application of the QM(DFT)/MM method on the catalytic mechanism of glycosyltransferases.

2. Computational Details

The Enzyme−Substrate Initial Structure. The 1.8 Å resolution crystallographic structure[11] of the catalytic fragment of rabbit GnT-I

(10) Nishikawa, Y.; Pegg, W.; Paulsen, H.; Schachter, H. *J. Biol. Chem.* **1988**, *263*, 8270−8281.
(11) Unligil, U. M.; Zhou, S.; Yuwaraj, S.; Sarkar, M.; Schachter, H.; Rini, J. M. *EMBO J.* **2000**, *19*, 5269−5280.
(12) Gordon, R. D.; Sivarajah, P.; Satkunarajah, M.; Ma, D.; Tarling, C. A.; Vizitiu, D.; Withers, S. G.; Rini, J. M. *J. Mol. Biol.* **2006**, *360*, 67−79.
(13) Tvaroška, I.; Andre, I.; Carver, J. P. *Glycobiology* **2003**, *13*, 559−566.
(14) Tvaroška, I. *Trends Glycosci. Glycotechnol.* **2005**, *17*, 177−190.
(15) Tvaroška, I.; André, I.; Carver, J. P. *J. Am. Chem. Soc.* **2000**, *122*, 8762−8776.
(16) Charnock, S. J.; Davies, G. J. *Biochemistry* **1999**, *38*, 6380−6385.
(17) Gastinel, L. N.; Cambillau, C.; Bourne, Y. *EMBO J.* **1999**, *18*, 3546−3557.
(18) Ha, S.; Walker, D.; Shi, Y. G.; Walker, S. *Protein Sci.* **2000**, *9*, 1045−1052.
(19) Kakuda, S.; Shiba, T.; Ishiguro, M.; Tagawa, H.; Oka, S.; Kajihara, Y.; Kawasaki, T.; Wakatsuki, S.; Kato, R. *J. Biol. Chem.* **2004**, *279*, 22693−22703.
(20) Mulichak, A. M.; Losey, H. C.; Lu, W.; Wawrzak, Z.; Walsh, C. T.; Garavito, R. M. *Proc. Natl. Acad. Sci. U.S.A.* **2003**, *100*, 9238−9243.
(21) Mulichak, A. M.; Losey, H. C.; Walsh, C. T.; Garavito, R. M. *Structure* **2001**, *9*, 547−557.
(22) Pedersen, L. C.; Tsuchida, K.; Kitagawa, H.; Sugahara, K.; Darden, T. A.; Negishi, M. *J. Biol. Chem.* **2000**, *275*, 34580−34585.
(23) Ramakrishnan, B.; Qasba, P. K. *J. Mol. Biol.* **2001**, *310*, 205−218.
(24) Mulichak, A. M.; Lu, W.; Losey, H. C.; Walsh, C. T.; Garavito, R. M. *Biochemistry* **2004**, *43*, 5170−5180.

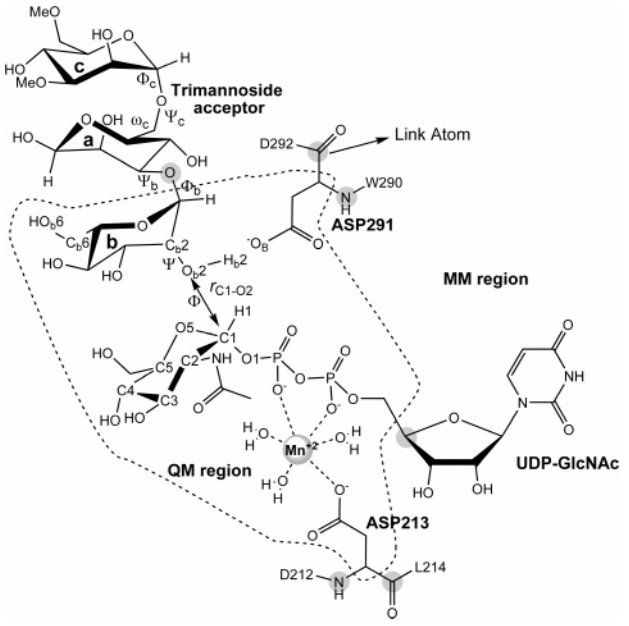

Figure 2. Schematic representation of the active site partitioning into QM and MM regions for the QM(DFT)/MM calculations. The QM region represented in this figure contains 88 atoms. The six linked atoms are indicated as gray ●.

in complex with UDP-GlcNAc (PDB code: 1FOA) was used to build our theoretical model. Starting from the X-ray structure of the enzyme−donor complex, hydrogen atoms were added, and all water molecules except 11 waters in the enzyme active site were removed. Because the available structures of GnT-I complexes have no acceptor, the first step in an investigation of the GnT-I reaction mechanism required determination of the binding mode for the acceptor. The missing acceptor was inserted using the docking procedure implemented in the Glide program from Schrödinger Inc.[25] As the acceptor, we used the trimannosyl core Manα1−3(3,6-OMe-Manα1−6)Manβ of the Man_5-$GlcNAc_2$−Asn−X oligosaccharide, which represents the minimal acceptor binding determinant.[26] The trimannoside acceptor was docked into the X-ray crystallographic structure of GnT-I in complex with UDP-GlcNAc. The result of this docking was a cluster of structures. The 0.5 Å maximum rms and 1.3 Å maximum displacement criteria were used during the docking procedure. Based on the estimated score, the best 100 docked poses were given further consideration. Their analysis showed four main binding modes having an approximately similar population of 25%. An inspection of their geometry revealed that the nucleophilic O_b2 atom of the acceptor is in suitable positions for the catalytic reaction in one of these binding modes. The pose having the O_b2-C1 and O_b2-O_B distances of 3.48 and 2.59 Å, respectively, was therefore selected as the starting structure. This structural model, containing 5721 atoms, was used to explore the mechanism of the enzymatic reaction of GnT-I as well as the role of interactions between the substrates and the enzymatic environment.

QM(DFT)/MM Model. The hybrid QM/MM treatment was carried out by means of the Amsterdam Density Functional (ADF) program system, ADF 2005.01.[27,28] The entire enzyme−substrate system, consisting of 341 amino acids, 11 water molecules, donor, acceptor, and a manganese cation (5721 atoms), was partitioned into two different subsystems: the QM and the MM regions. Figure 2 illustrates the QM/MM division of the active site and the numbering used for some relevant atoms. The QM subsystem was treated using the density functional theory (DFT) with the Becke−Perdew (BP) functional.[29,30] The atomic orbitals were taken from ADF library[28] and described as uncontracted triple-ζ Slater function basis sets, with a single-ζ polarized function on all atoms (TZP). The MM subsystem was characterized by the AMBER95 all-atom force field.[31]

The QM subsystem, containing 88 atoms, is formed by all essential moieties of the donor and acceptor substrates, the metal cofactor, and moieties of key amino acids involved either in the enzymatic reaction or in binding of the substrates. Thus, the QM part of the reaction site model (Figure 2) includes the DP-GlcNAc portion of the sugar-donor molecule; the Manα1−3 mannose residue (Man_b) of the trisaccharide acceptor, aspartate D291, the divalent metal cofactor Mn^{2+} fully coordinated by three water molecules (HOH 38, 87, 116), and aspartate D213 as found in the X-ray structure.[11]

The MM region is composed by the rest of the substrates and GnT-I atoms presented in the crystallographic structure. Six hydrogen link atoms were added to satisfy the valence of the QM fragments.[32] For our calculations, not only the QM atoms but also all of the MM atoms were free to relax during the investigation of the reaction mechanism. Prior to the potential energy surface calculations, a geometry optimization of the whole system was performed to acquire a refined location of the acceptor.

Reaction Mechanism. The reaction that GnT-I catalyzes is the formation of one new glycosidic linkage between the acceptor and donor, cleavage of the donor glycosidic linkage, and removal of a proton from the acceptor nucleophile. The reaction mechanism was monitored by the reaction coordinate r_{C1-O2}, defined as the distance between the anomeric carbon C1 and the oxygen O_b2 of the acceptor hydroxyl group (Figure 2). The employed reaction coordinate represents the nucleophilic attack of the oligosaccharide acceptor on the anomeric carbon of the donor UDP-GlcNAc. This selection of the reaction coordinate does not specifically assign the reaction coordinate for the breaking linkage or for the proton transfer, as suggested by our previous calculations of inverting glycosyltransferases.[13,15] The reaction path energy profile was determined by adiabatic mapping. The reaction coordinate r_{C1-O2} was varied by 0.2 Å increments, between 3.2 and 1.45 Å. All of the geometrical variables were optimized except the reaction coordinate. Once the energy profile was obtained, the structure of the energetic maximum was used to search for the transition state (TS) using default criteria for this type of computation in the ADF program system. The refined structure of the transition state was characterized by the frequency computation on the QM part of the system. The frequency calculation procedure of the ADF program was found inefficient for our system; therefore, the frequency calculations were performed at the DFT level of theory, with BP functional and the 6-31+G* basis set using PQS ab initio software.[33] Finally, the intrinsic reaction coordinate (IRC) path was traced back from the refined transition-state structure to the Michaelis complex (ES) and product complex (PC) using the 0.2 Å step size and default criteria of the ADF program system.

To ascertain the validity of the reaction mechanism, we have carried out calculations of the theoretical α-secondary deuterium kinetic isotope effect (KIE) for the catalytic reaction of GnT-I. These calculations were performed only on the QM part of the QM/MM refined structures of the ES and TS models. The frequency calculations for particular structures were performed at the DFT level of theory, with BP functional

(25) Schrödinger, I. *First Discovery 2.7*; Portland, OR, 2004.
(26) Schachter, H.; Reck, F.; Paulsen, H. *Methods Enzymol.* **2003**, *363*, 459−475.
(27) SCM. *ADF 2005.01*; Amsterdam, 2005.
(28) Te Velde, G.; Bickelhaupt, F. M.; Baerends, E. J.; Fonseca Guerra, C.; Van Gisbergen, S. J. A.; Snijders, J. G.; Ziegler, T. *J. Comput. Chem.* **2001**, *22*, 931−967.
(29) Becke, A. D. *Phys. Rev. A* **1988**, *38*, 3098−3100.
(30) Perdew, J. P. *Phys. Rev. B* **1986**, *33*, 8822−8824.
(31) Cornell, W. D.; Cieplak, P.; Bayly, C. I.; Gould, I. R.; Merz, K. M.; Ferguson, D. M.; Spellmeyer, D. C.; Fox, T.; Caldwell, J. W.; Kollman, P. A. *J. Am. Chem. Soc.* **1995**, *117*, 5179−5197.
(32) Swart, M. *Int. J. Quantum Chem.* **2003**, *91*, 177−183.
(33) Solutions, P. Q. *PQS Ab Initio Program Package v3.2*; Fayetteville, AR, 2006.

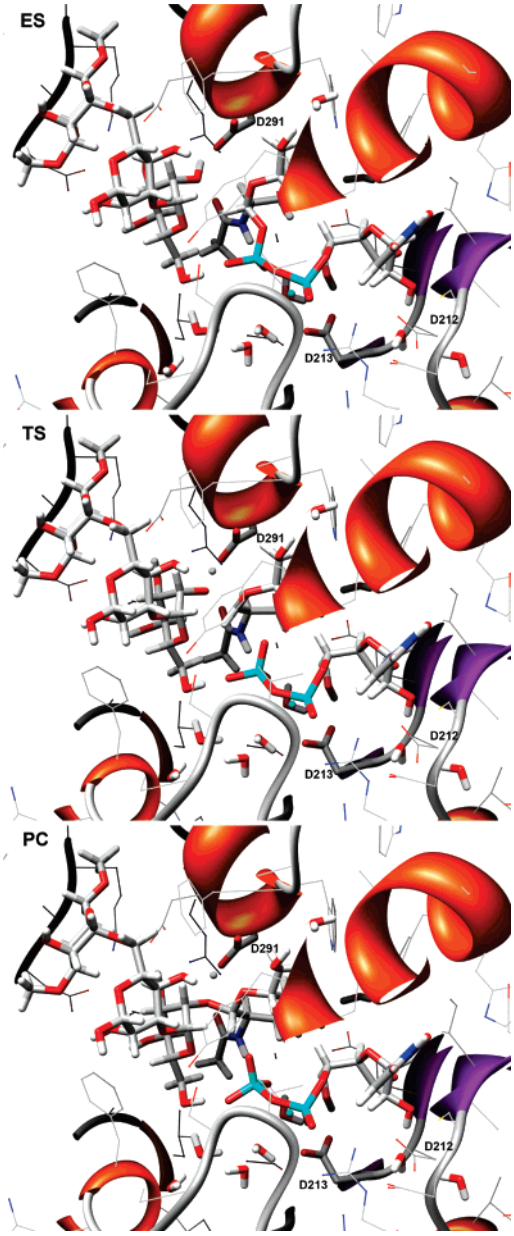

Figure 3. The active site models for the Michaelis complex (ES), transition state (TS), and the product complex (PC) obtained using the QM(DFT)/MM method.

and the 6-31+G* basis set using PQS ab initio software.[33] The appropriate α-secondary deuterium KIE was calculated using standard procedures.[34]

3. Results and Discussion

The QM/MM result of a minimal energy profile along the selected reaction coordinate suggests, similar to that of the truncated DFT model,[13] a concerted S_N2-type mechanism. The intrinsic reaction coordinate calculations led directly to the Michaelis complex in one direction and to the product complex in the other, further confirming the concerted nature of the reaction. The optimized structures of the active site models in the ES, TS, and PC complexes are shown in Figure 3, and some relevant geometric parameters of these stationary structures are listed in Table 1. The Cartesian coordinates of the QM(DFT)/MM optimized stationary points are included in the Supporting Information. A geometrical representation of the TS model is given in Figure 4, and the proposed reaction mechanism based on these results is shown in Figure 5.

Table 1. Relevant Geometric Parameters[a] of Stationary Structures Obtained at the QM(DFT)/MM Level of Theory Using the BP/TZP Basis Set

	R	TS	PC
$C1-O_b2$	2.974	1.912	1.431
O_b2-O_B	2.592	2.399	2.592
C1−O1	1.458	2.542	2.988
C1−O5	1.403	1.333	1.434
O_b2-H_b2	1.001	1.313	1.657
O_b2-O5	3.122	2.635	2.293
H_b2-O_B	1.677	1.122	1.014
C2−C1−H1	110.7	118.1	109.8
O5−C1−H1	107.9	115.4	110.4
O5−C1−C2	110.2	120.4	113.3
$O1-C1-O_b2$	156.6	157.0	131.8
C1−O1−P	123.0	116.8	122.2
C1−O5−C5−C4	49.4	24.4	54.6
$O1-C1-O_b2-C_b2$	24.1	30.3	33.6

[a] Distances are given in angstroms; angles are given in degrees.

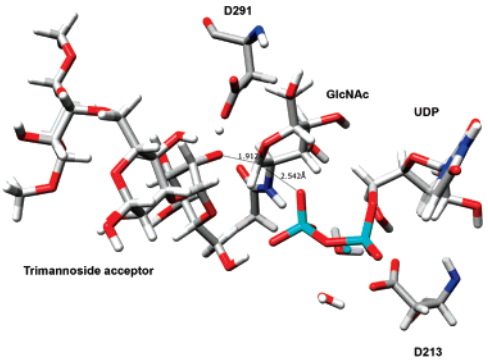

Figure 4. The geometrical representation of the donor and acceptor in the transition-state (TS) model obtained using the QM(DFT)/MM method.

Stationary Structures. The structure of the Michaelis complex (ES) model was determined from TS using the IRC path. The enzyme−donor part of the optimized structure of ES (Figure 3) was found to have a geometry almost identical to that reported for the crystallographic structure, and all of the enzyme−donor interactions within the GnT-I active site were conserved. The trimannoside acceptor is located in the binding site created by the structured 318−330 loop and is properly positioned for the nucleophilic attack on C1 of the donor. It appears that the position of trimannoside is in good accordance with the crystallographic position of the acceptor substrate analogue determined experimentally[22] for glucuronyltransferase I that belongs to the same GT-2 SpsA superfamily. The overall shape of bound trimannoside is bent, and its conformation can be described by a set of five glycosidic dihedral angles, $\Phi_b = \Phi_b(O_b5-C_b1-O_b1-C_a3)$, $\Psi_b = \Psi_b(C_b1-O_b1-C_a3-C_a2)$, $\Phi_c = \Phi_c(O_c5-C_c1-O_c1-C_a6)$, $\Psi_c = \Psi_c(C_c1-O_c1-C_a6-C_a5)$, and $\omega_c = \omega_c(O_c1-C_a6-C_a5-O_a5)$ with values of 140°, −171°, 152°, 114°, and −87°, respectively. The bound conformation of trimannoside differs from the conformation predicted for this trisaccharide by molecular dynamic simulations of the Man_3-$GlcNAc_2$.[35] The predicted conformation for trimannoside in

(34) Alvarez, F. J.; Schowen, R. L. *Mechanistic Deductions from Solvent Isotope Effects*; Elsevier: Amsterdam, 1987; pp 1−60.

(35) Balaji, P. V.; Qasba, P. K.; Rao, V. S. R. *Int. J. Biol. Macromol.* **1996**, *18*, 101−114.

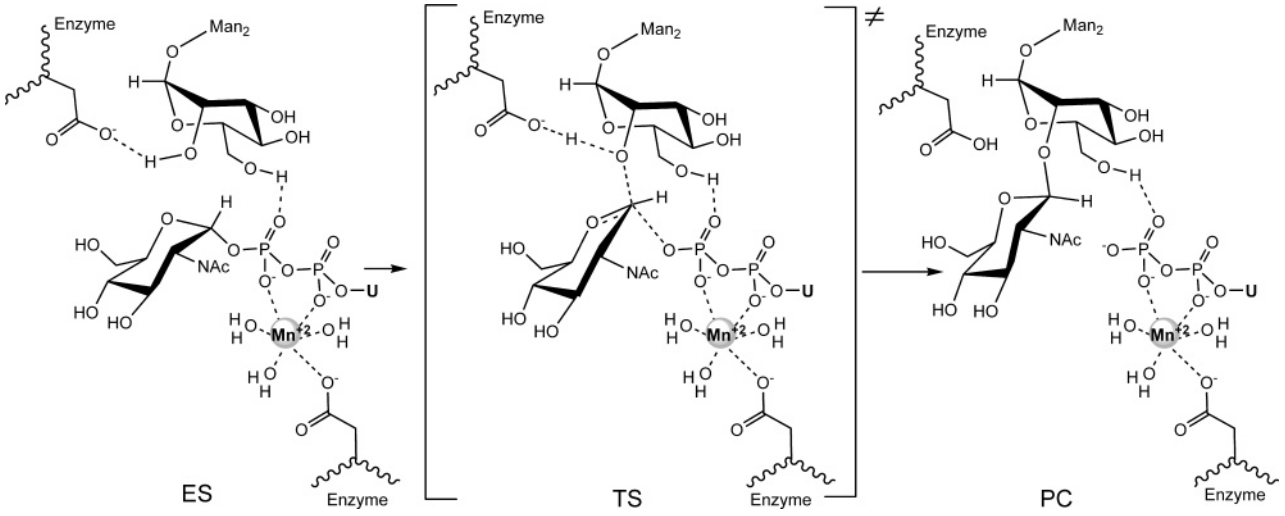

Figure 5. Schematic representation of the proposed mechanism for the GlcNAc transfer catalyzed by GnT-I.

aqueous solution was characterized by corresponding dihedral angles of 44°, −77°, 107°, 93°, and −77°, respectively. This difference is understandable and indicates that the enzyme has a tendency to bind substrates with conformation suitable for the catalytic reaction, and the bound conformation does not have to correspond to the most stable conformation in solution. To estimate the energy difference between the bound and free trisaccharide conformation, we have carried out a geometry optimization of the latter at the BP/TZP level with constrained glycosidic dihedral angles. The result showed that the bound trisaccharide has a higher energy of approximately 27 kcal/mol. The calculated value of the energy difference between the bound and free trisaccharides is very approximate, and a more accurate estimate would require a thorough conformational analysis of trisaccharide at the BP/TZP level including solvent effects, which is out of the scope of this paper.

The Man_b residue is buried deep in the binding site in the vicinity of GlcNAc and D291, while the Man_a and Man_c residues are positioned over Man_b, with the Man_a residue quite solvent-exposed. This is also reflected in a number of interactions between GnT-I and the acceptor residues. An analysis of these interactions shows that all hydroxyl groups on the α1,3-linked mannose (Man_b) are positioned to interact with the enzyme, or donor, and create a total of five hydrogen bonds. The crucial aspect of the catalytic mechanism is the position of a nucleophile, the C_b2 hydroxyl group. A distance of 2.97 Å between the nucleophile O_b2 and the anomeric carbon C1 of the donor is such that O_b2 oxygen is in an appropriate position for the nucleophilic attack. The O_b2-O5 distance is 3.12 Å, close to that observed[36] in the modeled crystal structure of β-1,4-galactosyltransferase I (GalT-I) and in the crystal structure of GnT-I with modeled Man_b moiety.[12] The calculated O_b2-O5 distance (3.12 Å), although similar to the O_b2-C1 distance of 2.97 Å, supports a recent proposal[36] that electrostatic repulsion, between the nucleophilic hydroxyl group oxygen of the acceptor and the ring oxygen O5 of the donor, might facilitate a distortion of the ring from the $^4C_1$ conformation to the $^4H_3$ conformation in the procession from the Michaelis complex to the TS. The O_b2 hydroxyl group also makes the key hydrogen bond with the carboxylate oxygen O_B of D291. This interaction might be critical for the reaction because the D291 carboxylate has been proposed to act as the catalytic base.[11] The observed O_b2-O_B and H_b2-O_B distances of 2.592 and 1.677 Å, respectively, indicate a short, strong hydrogen bond (low-barrier hydrogen bond, LBHB).[37] The LBHB interaction facilitates deprotonation of the nucleophile and thereby increases the nucleophilicity of O_b2. The C_b6 hydroxyl makes hydrogen bonds to both the β-phosphate oxygen of the UDP-GlcNAc and the water molecule HOH14 placed in the active site of the enzyme. The corresponding distances are 1.79 and 1.63 Å. The ES structure also shows hydrogen bonds between the C_b3 and C_b4 hydroxyl groups and D292 and R415, respectively. The binding mode of Man_b is supported by kinetic studies on substrate analogues.[26] These experiments showed that either removal or methylation of the C_b3 hydroxyl group leads to a loss of the enzyme activity. Similarly, the observation that removal of the C_b4 and C_b6 hydroxyl groups decreases the enzyme activity and that O_b6 methylated acceptor is tolerated as a substrate but has no catalytic activity is consistent with predicted hydrogen bonds for these hydroxyl groups. The regions around the C_b5 and C_b6 atoms are involved in hydrophobic interactions with F326 and L331.

The central mannose residue (Man_a) of the trisaccharide acceptor is located in the hydrophobic pocket formed by three amino acids residues Y181, Y184, and F289. This type of hydrophobic interaction, between carbohydrates and enzymes, is quite common for many glycosyltransferases and glycosylhydrolases[38] and may serve as an anchor for proper orientation of the acceptor. The β-linked O_a1 hydroxyl group is not involved in any hydrogen bond and is quite solvent-exposed. This is consistent with the fact that the O_a1 is linked to the $GlcNAc_2$ part of the $Man_5GlcNAc_2$–Asn-containing native substrates (Figure 1). The α1,6-linked mannose (Man_c) is positioned on the top of the active site and is solvent-exposed. An analysis of docked poses indicates that the Man_c residue is the most flexible residue and can adopt several different orientations. The Man_c orientation, therefore, represents only the local minimum nearest to the starting docking pose. This suggests that the orientation

(36) Ramakrishnan, B.; Ramasamy, V.; Qasba, P. K. *J. Mol. Biol.* **2006**, *357*, 1619−1633.
(37) Frey, P. A.; Whitt, S. A.; Tobin, J. B. *Science* **1994**, *264*, 1927−1930.
(38) Muraki, M. *Protein Pept. Lett.* **2002**, *9*, 195−209.

of this residue might be more influenced by the presence of residues linked to the trisaccharide in native substrates when compared to Man_a or Man_b. To ascertain the validity of the bound position of Man_3, we carried out some docking calculations with $Man_3GlcNAc_2$. Our preliminary results, on the docking of $Man_3GlcNAc_2$ oligosaccharide into the GnT-I active site, show that while the Man_a or Man_b residues are bound in the same fashion, the orientation of the Man_c residue in $Man_3GlcNAc_2$ is slightly different. A comparison of Man_3 and $Man_3GlcNAc_2$ binding modes revealed that they both differ from the recently proposed position of the Manα1,3Manβ1 disaccharide.[12] This is understandable because the rigid conformation of a disaccharide, described by a set of two glycosidic dihedral angles, $\Phi = 50°$ and $\Psi = -120°$, used to build their model differs from the optimized conformation ($\Phi_b = 140°$, $\Psi_b = -171°$) in the Michaelis complex (ES) model. Attempts to superimpose the trisaccharide with the modeled disaccharide were unsuccessful due to steric interactions of the third mannose residue Man_c with the enzyme.

The structure of the active site in the TS model is displayed in Figures 3 and 4, and its relevant geometrical parameters are listed in Table 1. The QM(DFT)/MM results suggest a concerted S_N2-type of transition state with D291 as the catalytic base. The TS was located at the reaction coordinate r_{C1-O2} equal to 1.912 Å and features nearly simultaneous nucleophilic addition and dissociation steps, as evidenced by a shortened O_b2-C1 bond (1.912 Å versus 2.974 Å in the ES complex) and elongated C1−O1 bond (2.542 Å versus 1.431 Å in the ES complex). The normal-mode analysis of the QM part of the transition-state model shows one strong imaginary frequency at −259.7 cm^{-1}, with direction vectors corresponding to the breaking and forming glycoside bonds, which corroborates the transition-state geometry. As the nucleophile oxygen O_b2 approaches C1, its hydrogen atom (H_b2) starts to move toward O_B of the catalytic base D291. The O_b2-O_B, O_b2-H_b2, and O_B-H_b2 distances at the TS are 2.399, 1.313, and 1.122 Å, respectively. In the ES, the corresponding distances are 2.592, 1.001, and 1.657 Å, respectively. In the procession from the ES complex to the TS, as expected, the major movements can be observed for the acceptor and for the transferred GlcNAc. The glucopyranose ring adopts the standard $^4C_1$ conformation in the ES model. In the $^4H_3$ conformation adopted in the TS model, the sum of the bond angles around the C1 is 354° and shows that C1 is essentially planar. As a result, the anomeric hydrogen H1 is positioned in the plane defined by C1, C2, and O5 atoms. This arrangement facilitates co-incident interactions of the C1 with the leaving O1 and nucleophile O_b2. The C1−O5 distance is shortened in the TS (1.333 Å versus 1.403 Å in the ES complex). This points to a significant delocalization of the O5 lone pairs to C1 and results in a partial double-bond character of the bond between the ring oxygen and the anomeric carbon. Obviously this delocalization stabilizes the partial positive charge on the anomeric carbon C1 within the oxocarbenium ion-like character of the TS. The distance between the H_b6 and β-phosphate oxygen (1.66 Å) indicates strong interactions that, together with the participation of the hydrogen from the S322 side chain hydroxyl group, stabilize the building of a negative charge on the β-pyrophosphate. The cleavage of the C1−O1 glycosidic bond is accompanied by the 17° rotation of the β-phosphate oxygen on going from the ES to TS complex, while the remaining part of UDP does not show any relevant changes. A similar conformational change of the β-phosphate oxygen during a cleavage of the anomeric linkage was experimentally observed[36] for β-1,4-galactosyltransferase I, and one can only speculate as to whether this kind of conformational change is characteristic for inverting glycosyltransferases.

The transition-state structures for glycosyltransferases have been recently divided into three canonical groups using distances between the anomeric carbon C1 and nucleophile oxygen (O_{Nuc}), and between C1 and O1, respectively.[14] The first group is characterized by long C1−O_{Nuc} bonds within the range of 2.4−2.7 Å, and short C1−O1 distances between 1.5 and 2.1 Å. The geometrical parameters of this transition-state model are similar to the initial reactants, and this canonical form has been termed as the "early transition state". The second group corresponds to the "intermediate transition-state" structures where both C1−O_{Nuc} (2.1−2.4 Å) and C1−O1 (2.5−2.7 Å) distances are elongated as compared to their initial values, but the structures have not yet reached the final arrangement observed in the products. The third group is characterized by short C1−O_{Nuc} bonds within the range of 1.4−1.6 Å, and long C1−O1 distances between 2.8 and 3.2 Å. The geometry of this canonical form is close to that of final products, and therefore this model has been named as the "late transition state". The QM(DFT)/MM results indicate that the structure of TS model might correspond to the so-called "intermediate transition state". The geometrical parameters of the QM(DFT)/MM transition-state model are similar to the parameters previously calculated[13] for the DFT truncated model of TS. Although this agreement is not perfect, both models suggest the same catalytic mechanism for GnT-I.

The product complex (PC) model (Figure 3 and Table 1) features a complete transfer of GlcNAc to the acceptor. The newly formed β-glycosidic linkage is indicated by the C1−O_b2 distance of 1.431 Å. The C1−O1 distance increased to 2.988 Å, reflecting the cleavage of this bond. The catalytic base D291 is protonated, and the O_b2-O_B distance increased back to 2.6 Å. In the PC complex, the glucopyranose ring adopts the standard $^4C_1$ conformation and GlcNAc orientation, and with respect to the trisaccharide is characterized by two glycosidic dihedral angles $\Phi = -81°$ and $\Psi = -27°$. This orientation belongs to the main conformational region inferred from molecular dynamic simulations of $GlcNAcMan_3GlcNAc_2OMe$ oligosaccharide[39] and centered around (−60°, −60°).

The catalytic mechanism of GnT-I, which has emerged from both the truncated DFT and the QM(DFT)/MM models, is illustrated in Figure 5. As mentioned earlier, this mechanism suggests a concerted S_N2-type mechanism featuring a nearly simultaneous nucleophilic addition of the O_b2 oxygen from Man_b to the C1 carbon of GlcNAc, as well as dissociation of the C1−O1 bond of UDP-GlcNAc accompanied by the transfer of H_b2 proton from nucleophile to the catalytic base D291. The calculated energy barrier for the proposed mechanism (Figure 5) is 18.7 kcal mol^{-1}, and the PC model is 4.4 kcal mol^{-1} less stable than the ES model. The calculated QM(DFT)/MM energies ΔE and their decomposition, with the contribution from the MM part of energy ΔE_{MM} and from the QM part of the energy ΔE_{QM}, are listed in Table 2. The calculated barrier along the proposed reaction path ES → TS → PC is consistent within

(39) Kožár, T.; Tvaroška, I.; Carver, J. P. *Glycoconjugate J.* **1998**, *15*, 187−191.

Table 2. QM(DFT)/MM Relative Energies (kcal mol^{-1}) of the Stationary Structure Models for the Transfer of GlcNAc Residue Catalyzed by GnT-I

energetics	TS	PC
ΔE	18.74	4.41
ΔE_{MM}	−8.82	−1.70
ΔE_{QM}	27.56	6.11

Table 3. Energetics (kcal mol^{-1}) for Calculations of the α-Secondary Kinetic Isotope Effect (KIE) Using the QM Part of Active Site Models

energetics	TS(H1)	TS(D1)
ΔE	28.186	28.186
ΔZPE	2.194	2.157
ΔH	2.007	1.957
ΔS^a	−2.126	−2.177
ΔG	2.641	2.606
calculated α-secondary KIE	1.060	

[a] Entropy contribution in cal K^{-1} mol^{-1}.

the experimentally observed barriers[40] of 15−25 kcal mol^{-1}. This coincidence, however, is likely to be superficial. A comparison of individual energetic contributions revealed that ΔE_{QM} for both the TS and the PC complexes is higher as compared to ΔE. However, the ΔE_{MM} contribution is decreasing the overall energetic barrier by 8.8 kcal mol^{-1} and indicates that the GnT-I environment is favoring the TS and PC complexes over the ES complex.

The QM(DFT)/MM calculations indicate various ways in which the GnT-I environment is involved in the catalytic reaction. In the ES complex, the acceptor is placed in the active site in such a way that nucleophile oxygen O_b2 is properly positioned for the nucleophilic attack and for the activation by the catalytic base D291. The O_b2 atom is at a distance of 3.0 Å from C1 of the donor and of 2.6 Å from the catalytic base oxygen. Moreover, an orientation of the nucleophile and leaving group oxygen atoms, characterized in the case of GnT-I by the O1−C1−O_b2 angle, is in the ES complex 157°. This represents almost the ideal angle for the nucleophilic attack. A comparison of the stationary structures revealed that GnT-I adopts to movements of the substrates. However, we were able to identify only two specific interactions that could be responsible for a specific stabilization in the TS model, LBHB between the H_b2 and O_B and strong interactions between the hydrogen atom H_b6 and β-phosphate oxygen (indicated by a distance of 1.66 Å) that together with the hydrogen from S322 side chain hydroxyl group stabilize the building of a negative charge on the β-pyrophosphate.

To ascertain the proposed mechanism, we have calculated the α-deuterium kinetic isotope effect using the QM part of the calculated ES and TS complexes. The calculated vibrational frequencies are included in the Supporting Information. The calculated results are given in Table 3. Experimentally observed α-^{2}H KIE for inverting glycosyltransferases varies in the interval $D_{V/K} = 1.050-1.210$.[41−45] The calculated α-^{2}H KIE value of 1.060 is in the range of experimental values. When the reaction mechanism proceeds via the pure S_N2 mechanism, the value of the α-^{2}H KIE is in the range 1.000−1.030; and for the reaction involving glucopyranosyl cation as an intermediate, the KIE value is in the interval of 1.130−1.380.[41,42] Our calculated KIE value is slightly higher than the experimentally measured KIE for the S_N2 mechanism, but is also considerably lower than KIE for the reactions corresponding to the S_N1 mechanism. The calculated values may suggest that in the catalytic reaction the nucleophilic addition and dissociation of the glycosidic bonds occurs nearly synchronously, like in the S_N2 mechanism, without forming a covalent intermediate with enzyme. Similar mechanistic features were observed for a dissociative S_N2 mechanism (or A_ND_N) of the purine nucleoside phosphorylase,[46] in which the distances of the making and breaking bond are not symmetrical in the transition state and the length of the breaking bond is longer as compared to the forming bond.

4. Conclusions

The present results shed some light on the catalytic mechanism of the *N*-acetylglucosamine (GlcNAc) transfer by the inverting *N*-acetylglucosaminyltransferase I (GnT-I) and suggest a concerted reaction mechanism involving oxocarbenium ion-like TS. The mechanism is characterized by the calculated reaction barrier of 18.7 kcal mol^{-1} at the QM(BP/TZP)/MM-(Amber95) level of theory, and by the predicted α-^{2}H KIE of 1.060. These results are in a fair agreement with experimental values. The structure of TS is characterized by the C1−O1 bond elongated to about 2.5 Å and the C1−O_b2 distance shortened to about 1.9 Å, which resembles the geometry of the "intermediate transition state". These results, together with the analysis of the models for the ES, TS, and PC complexes, led us to suggest that the GnT-I environment influences the catalytic reaction by imposing a correct orientation of substrates in the Michaelis complex and that interactions between the nucleophile and catalytic base D291 and between the H_b6 and β-phosphate oxygen of the UDP contribute to a stabilization of TS. The obtained information about the structure of TS is essential for the design of transition-state analogue inhibitors for glycosyltransferases.

Acknowledgment. This work was supported by grants from the Mizutani Foundation for Glycoscience (no. 040013) and from the Science and Technology Assistance Agency under contract no. APVT-51-04204.

Supporting Information Available: Cartesian coordinates of the QM(DFT)/MM optimized structures, the ES, TS, and PC complexes, and vibrational frequencies calculated for the QM region. This material is available free of charge via the Internet at http://pubs.acs.org.

JA065944O

(40) Seto, N. O. L.; Compston, C. A.; Evans, S. V.; Bundle, D. R.; Narang, S. A.; Palcic, M. M. *Eur. J. Biochem.* **1999**, *259*, 770−775.
(41) Kim, S. C.; Singh, A. N.; Raushel, F. M. *J. Biol. Chem.* **1988**, *263*, 10151−10154.
(42) Kim, S. C.; Singh, A. N.; Raushel, F. M. *Arch. Biochem. Biophys.* **1988**, *267*, 54−59.
(43) Murray, B. W.; Takayama, S.; Schultz, J.; Wong, C. H. *Biochemistry* **1996**, *35*, 11183−11195.
(44) Murray, B. W.; Wittmann, V.; Burkart, M. D.; Hung, S. C.; Wong, C. H. *Biochemistry* **1997**, *36*, 823−831.
(45) Werner, R. M.; Stivers, J. T. *Biochemistry* **2000**, *39*, 14054−14064.
(46) Lewandowicz, A.; Schramm, V. L. *Biochemistry* **2004**, *43*, 1458−1468.